


A composite monolithic column fabricated with functionalized nanodiamond and its application in separation of small molecules

Aile Wei^{1,2} · Peipei Dong^{1,2} · Beijiao Cui^{1,2} · Fengqing Wang^{1,2} · Haiyan Liu^{1,2}  · Ligai Bai^{1,2} · Hongyuan Yan^{1,2}

Published online: 29 August 2016
© Springer Science+Business Media New York 2016

Abstract A nanodiamond-based composite monolithic column was fabricated by redox initiation for high performance liquid chromatography (HPLC). The functionalized nanodiamond was modified via Fenton Reagent and 3-methacryl oxypropyltrimethoxysilane (KH-570). After being optimized conditions, composite monolithic columns were prepared with functionalized ND (f-ND) as functional monomer, dipentaerythritol hexaacrylate and ethylene dimethacrylate as crosslinking agents, dodecanol and 1-propanol as co-porogens, dibenzoyl peroxide and N,N-dimethyl aniline as initiators. Characterizations of the resulting nanocomposite, including fourier transform infrared spectra, scanning electron microscopy images, thermal gravimetric analysis, mercury intrusion porosimetry and nitrogen adsorption–desorption isotherm were all carried out in detail. Bigger specific surface area, better mechanical stability, thermostability property and orderliness skeleton structure with flow-through channels and macroporous of the composite monolithic column was exhibited than those columns without f-ND added. At last, the nanodiamond-based composite monolithic column was used to separate a series of small molecules including acidic, alkaline and neutral compounds with good resolution and reproducibility in HPLC.

Keywords Nanodiamond · Composite · Polymer monolithic column · Separation of small molecules · High performance liquid chromatography

1 Introduction

Nanodiamond (ND), that is, diamond particles with a diameter smaller than 100 nm, has become one of the attractive member in the field of nanosized materials such as graphene oxide [1], carbon nanofiber and carbon nanotubes [2, 3]. Nanodiamond was created by nuclear explosions that used carbon-based trigger explosives by Russian scientists in the 1960s [4]. ND particles stimulate broad interest among science and industry [5] due to its excellent properties, including superior thermal conductivity, hardness, Young's modulus, high resistivity, chemical inertness, good electrical insulating and a high refraction index [6–10]. These outstanding properties are potentially suitable for diverse applications, for example Atsuhiko Fujimori's group has fabricated transparent and flexible crystalline polymer nanohybrid film containing well-dispersed nanodiamond filler [11].

Taking these attractive features into account, it is important that the surface of ND particles can be modified by a variety of functional groups, including hydroxyl group, carboxyl group, and lactone group [12–14]. ND particles can be combined with organic polymers forming polymer nanocomposite in order to optimize properties utilizing ND excellent characters [14]. ND composite has received considerable attention and applied in various fields. Yury Gogotsi and co-workers have studied that the nanodiamond-polymer composite films can provide UV protection and scratch resistance to a variety of surfaces [15]. Meng-Chih Su's group has reported the static

✉ Haiyan Liu
lhy1610@126.com

¹ Key Laboratory of Pharmaceutical Quality Control of Hebei Province, College of Pharmaceutical Sciences, Hebei University, Baoding 071002, China

² Key Laboratory of Medicinal Chemistry and Molecular Diagnosis, Ministry of Education, Baoding 071002, China

attachment of proteins onto ND providing a fundamental understanding for the use of NDs as a platform for nanomedical drug delivery [16].

During the past decades, monolithic stationary phases have been developed rapidly in high performance liquid chromatography for their advantages of simple preparation, low back pressure and versatile modes to be modified compared to conventional columns packed with particles [17, 18]. Particularly, the organic polymer monolith exhibits good stability to all pH values and has been used as stationary phase in the separation of macromolecules such as proteins and nucleic acids [19–22] but relative poor performance in the separation of small molecules.

In this work, a kind of f-ND based polymer composite monolithic columns were synthesized by a one-step redox initiation process, in which the modified ND particles were functionalized in lab. The f-ND based composite monolith column was applied for the separations of acidic, alkaline and neutral compounds achieving good performance without buffer by reversed phase high performance liquid chromatography.

2 Experimental

2.1 Reagents and chemicals

All reagents used were of analytical grade unless otherwise stated. DPHA was supplied by Liyang Runda Co. Ltd. (Liyang, China). EDMA and KH-570 was purchased from Macklin Co. Ltd. (Shanghai, China). ND (50 nm) was produced by Xuzhou Jiechuang New Material Technology Co. Ltd. (Xuzhou, China). BPO, acetone, dodecyl alcohol, $\text{FeSO}_4 \cdot \text{H}_2\text{O}$, H_2O_2 , H_2SO_4 and ethanol were obtained from Tianjin Guangfu Chemical Co. Ltd. (Tianjin, China). Propanol, DMA and HPLC-grade methanol were products of Kermel Chemical Reagent Co. Ltd. (Tianjin, China). Aromatic compounds were purchased from Beijing Chemical Plant (Beijing, China). Ultrapure water was prepared using a Millipore-Q water-purification system (Taiwan, China) and all solutions were filtered through a 0.45 μm membrane. The stainless-steel columns (50 \times 4.6 mm i.d.) were obtained from Beijing Xinyu Instrument Co. Ltd. (Beijing, China).

2.2 Apparatus

All chromatographic experiments were performed on a Dionex UltiMate 3000 from Thermo Fisher Scientific. Scanning electron microscopy (SEM) of the monolithic columns was carried out on a KYKY-2800B SEM scanning electron microscope (Beijing, China). Fourier transform infrared spectrum (FTIR) of ND, h-ND and f-ND were

recorded on a FTIR-8400S IR apparatus in the region of 400–4000 cm^{-1} (Shimadzu, Kyoto, Japan). Thermogravimetric (TGA) measurements were performed on a Setsys 16/18 (Setaram, Caluire, France). X-ray powder diffraction (XRD) was carried out using an X-ray powder diffractometer (D8 ADVANCE, Bruker/Switzerland). The porous property of f-ND based polymer composite was investigated by mercury intrusion porosimetry (MIP) on an AutoPore IV 9500 (Micromeritics, USA). The surface area was performed by nitrogen adsorption–desorption on a Tristar II 3020 (Micromeritics, USA).

2.3 Preparation section

2.3.1 Surface modification of nanodiamond

Firstly, hydroxylated ND (h-ND) was prepared using Fenton reagent (hydrogen peroxide and FeSO_4). Briefly, $\text{FeSO}_4 \cdot \text{H}_2\text{O}$ (6.95 g) was dissolved in ultrapure water and adjusted to pH 3 using H_2SO_4 . Next, ND (0.1 g) and H_2O_2 (42.5 g) were mixed in the solvent above and refluxed for 5 h at 80 °C. After that, h-ND were separated by centrifuge and washed with water for several times to pH 6–7 and dried under vacuum for further use.

Secondly, the same weight of h-ND and KH570 were mixed with 30 mL 95 % (v/v) ethanol and reacted 6 h at 60 °C equipped with mechanical stirrer and thermometer. Next, the f-ND were separated by centrifuge and washed with acetone in order to remove unreacted KH-570. At last, the f-ND were evacuated in vacuum at 80 °C for 12 h.

2.3.2 Preparation of nanodiamond-based polymer composite monolith

DPHA (100 mg), f-ND (2 mg), EDMA (0.6 mL) and BPO (5 mg) were dissolved in a binary porogenic solvent, which consisted of dodecanol (0.3 mL) and propanol (0.7 mL). The mixture solution was sonicated for 20 min after being shaken for 2 min and bubbled with nitrogen for another 5 min to obtain a homogeneous solution and remove gases. Then DMA (50 μL) was added in the mixture degassed with an ultrasonicator and was allowed to proceed at room temperature for 1.5 h. The scheme of polymerization was shown in Fig. 1.

2.4 Calculation

The ability of liquid passing the material was expressed by permeability, which reflected through-pore size and external porosity. The permeability (K) of monolithic columns was calculated by Darcy's Law:

$$K = F \times \eta \times L / \Delta P \times \pi \times r^2 \quad (1)$$

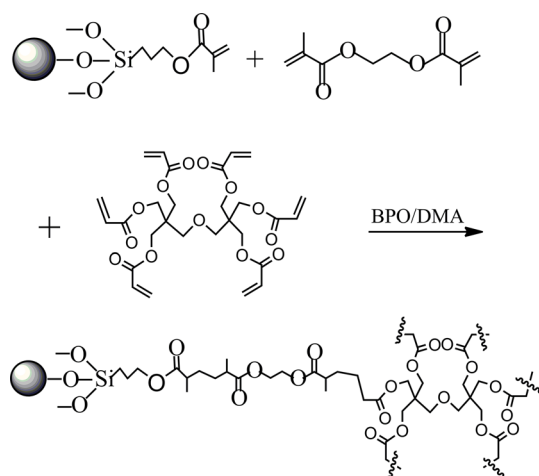


Fig. 1 Synthesis scheme of poly(ND-co-DPHA-co-EDMA) composite monolith

where F is the flow rate of the mobile phase, η is the dynamic viscosity of the mobile phase, L is the length of column, ΔP is the back pressure of the column, and r is the inner radius of the column [23]. In this work, methanol was used as mobile phase and its corresponding value of dynamic viscosity was 0.580 cP at 25 °C [24].

The retention factor (k) of each aromatic compound on poly (f-ND-co-DPHA-co-EDMA) monolith for HPLC separation was defined as the equation,

$$k = (t_R - t_0)/t_0 \quad (2)$$

where k , t_0 , t_R , stand for the retention factor, the retention time of aromatic compounds, and the retention time of void marker, respectively. Thiourea was selected as the void time marker in this experiment.

Theoretical plate number (N), one of the parameters of the chromatographic column efficiency, is a quantitative representation, which indicates the separation efficiency. An equation has been used to calculate the plate number:

$$N = 5.55(t_R/W_{0.5})/L \quad (3)$$

where N is the theoretical plate number per m, t_R is the retention time of the analyte in min, $W_{0.5}$ is the peak width at half height in min and L is the length of the column [25].

2.5 HPLC procedures

All chromatographic experiments were performed on a Dionex UltiMate 3000 from Thermo Fisher Scientific. All sample solutions injected in the chromatographic system were filtered through a Millipore membrane (0.45 μm) to remove particles and large aggregates. A flow rate of 1 mL/min was used unless otherwise stated and the UV absorbance was monitored at 254 nm. The sample injection volume of the autosampler was 10.0 μL .

3 Results and discussion

3.1 Preparation and optimization of the nanodiamond-based polymer composite monolithic column

3.1.1 Surface modification of nanodiamond

As known, the pristine ND particles tend to agglomerate because of large surface area, while the surface functional groups on the pristine ND tend to reduce the agglomeration. Various methods for the functional ND particles have been reported such as carboxylated, hydroxylated, hydrogenated, amination of the ND surface. In this work, highly efficient way for the direct establishment of OH groups on the ND surface consisted in the reaction of pristine ND with the so-called Fenton reagent which was made of hydrogen peroxide and FeSO_4 in strongly acidic solution. Then the h-ND reacted with KH570. After a series of experiments, the optimal reaction conditions such as temperature and time have been established.

3.1.2 Optimization of the f-ND based polymer composite monolithic column

Due to the good properties of the composite, it is expected that the f-ND based polymer composite could be used as stationary phase in HPLC. Several parameters which concern the polymerization such as the amount of monomer and crosslinker, the ratio of porogens have to be taken into account, since the composition of the reaction mixture has a great influence on the monolithic structure and column performance. A prepolymerization solution composition of monomer, crosslinking agents, porogens and initiator was listed in Table 1. In addition, the redox initiator which occurs quickly under contact pressure and ambient temperature conditions has several advantages: reduction the activation energy of organic peroxide decomposition, effective control of the reaction rate, complete curing reaction. The system generally consists of peroxide in combination with a reducing agent. Here, the reducing agent was N, N-dimethyl aniline. Benzoyl peroxide can initiate the polymerization of vinyl monomers. The complex decomposed and gave free radicals or cation radicals which could then initiate radical polymerization.

Porogens are important to obtain desired porous microstructure of a polymer monolith. It is generally accepted that good solvents serve as microporogens to provide high surface areas, while poor solvents act like macroporogens to provide good bulk flow properties. In this study, several porogenic solvents, including dodecyl alcohol, isopropyl alcohol, 1-propanol, polyethylene

Table 1 Compositions of the polymerization mixtures for the composite monolith prepared in this study

Columns	ND (mg)	DPHA (g)	EDMA (mL)	Dodecanol (mL)	1-Propanol (mL)	BPO (mg)	DMA (μ L)	Back pressure ^a (bar)	Permeability K ($\times 10^{-14} \text{m}^2$)
A	2	0.06	0.6	0.3	0.7	5	50	4	7.25
B	2	0.1	0.6	0.3	0.7	5	50	6	4.83
C	2	0.14	0.6	0.3	0.7	5	50	>12	–
D	0	0.1	0.6	0.3	0.7	5	50	3	9.667
E	3	0.1	0.6	0.3	0.7	5	50	No. dispersing of ND	–
F	2	0.1	0.6	0.18	0.82	5	50	>12	–
G	2	0.1	0.6	0.42	0.58	5	50	3	9.667

^a Back pressure is obtained with methanol as the mobile phase at 1 mL/min, and the length of the stainless steel column was kept at 5 cm

glycol, cyclohexanol and 1,4-butanediol, have been examined for their compatibility. A binary porogenic solvent containing 1-propanol which played an important role in forming micropore and dodecyl alcohol which tended to forming macropore was preferentially considered. Taking polarity into account, a binary porogenic was also the priority selection. This binary porogenic solvent could improve the compatibility of polymeric solution and allow the fine control of the porous properties of the resulting composite monolith over a wide range. As shown in Table 1, the content of 1-propanol less than 18 % had great difficult in dispersing f-ND; while the content of 1-propanol more than 42 % led to the obtained monolithic matrix becoming slack. Therefore, 30:70 (v/v) was finally chosen as the most suitable ratio of dodecyl alcohol: 1-propanol.

The monomer and crosslinker both play important roles in the preparation of the composite monolith. They have significant effects on not only the formation of monolithic skeleton, but also its chromatographic behaviors such as retention capability, peak symmetry and column efficiency. Here, DPHA belongs to polyolacrylate that can be used as important crosslinker. Compared with other crosslinker, DPHA possesses six double bonds with high reactivity, which can capture free radicals easily to form dense skeletal structure with EDMA. Three monolithic columns were prepared with the different ratios of f-ND/DPHA. With the increase of monomer, back pressure of the monolith gradually increased and permeability of the corresponding monolith decreased. Taken together, column B was chosen for further study.

3.2 Characterization

3.2.1 FT-IR

FTIR analysis was used to characterize the pristine ND, h-ND and f-ND particles. Figure 2a showed the FTIR

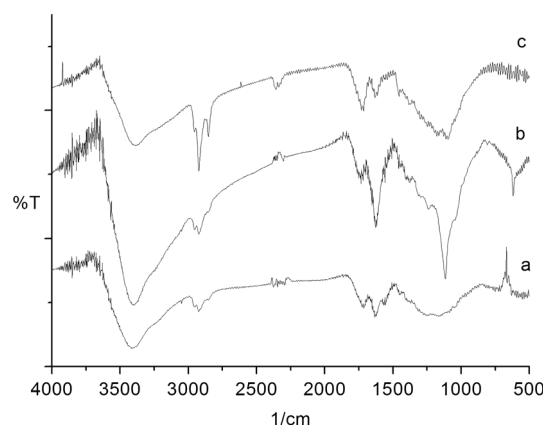


Fig. 2 a FT-IR spectra of pristine ND powder; b h-ND and c f-ND

spectrum of pristine ND powder. Compared to Fig. 2a, a significant absorption bands assigned as hydroxyl groups appeared in the spectra area of $3300\text{--}3500 \text{cm}^{-1}$ (O–H stretching vibration) and around 1620cm^{-1} (O–H bending vibration) was observed in Fig. 2b for h-ND. The peak at $1100\text{--}1200 \text{cm}^{-1}$ was identified stretching vibration of the C–O bond in C–OH and the peak around 1730cm^{-1} was corresponding to C=O stretching vibration in carbonyl, carboxyl groups. The band at 1620cm^{-1} can be assigned to stretching vibration of aromatic sp^2 carbon bond which can be related to graphite around the ND particles. The results proved that hydroxy was covalently bound to ND. In Fig. 2c for f-ND, the absorption bands around 2900cm^{-1} corresponding to C–H stretching in CH_2 of alkyl group became pronounced after functionalization of h-ND which confirmed that KH-570 was covalently bound to it. Moreover, the decrease of peak intensity at 3500 and 1120cm^{-1} revealed the consumption of hydroxy. The spectra area of $1200\text{--}1400 \text{cm}^{-1}$ is most likely to be connected with several band superpositions including asymmetric O–N vibration of R–O– NO_2 groups. This was due to the fact that the ND powder was produced by explosion

using trinitrotoluene and hexogen mixtures, the observed nitrogen may be the residue during producing process.

3.2.2 The thermostability and mechanical stability of the polymer composite

Figure 3a showed the TGA traces of polymer both with and without f-ND. As expected, TGA of the f-ND based polymer composite in weight loss was observed at 300 °C which was higher than polymer without f-ND in weight loss at 245 °C. This indicated that the ND particles could act as a barrier to hinder the volatile decomposition products throughout the composites. The result revealed that the thermal stability of polymer could be improved by the addition of the f-ND particles. This was in agreement with ND thermostability property.

It is important that the stationary phase of HPLC has good mechanical strength and permeability. In order to characterize the mechanical performance and permeability of the composite monolith, the back pressures at different flow rates with methanol and water as the mobile phase

were studied, respectively. Figure 3b showed excellent linear correlations ($r > 0.99$), which clearly indicated that the monolith column B was mechanically stable.

In addition, more than 50 injections were made to examine the stability of the column and the performance of the polymer composite was not reduced, which confirmed good mechanical stability of column B. In this work, the good permeability value of $4.83 \times 10^{-14} \text{ m}^2$ was calculated based on Darcy's Law, when the flow rate was 1.0 mL min^{-1} and methanol as mobile phase.

3.2.3 Morphology of polymer composite and pore size distribution

An impressive skeleton microstructure of the f-ND based composite polymer scanned with SEM was shown in Fig. 4a. SEM images illustrated a cage-like skeleton structure with the flow-through channels between aggregates of globules and the macroporous on those globules, which can be corroborated with the results of MIP in Fig. 4b. Two different pore sizes occurred and they were

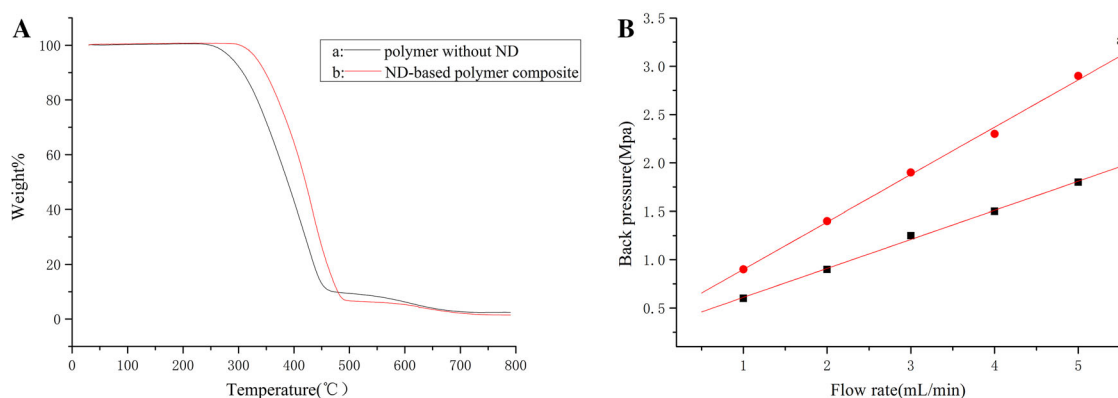


Fig. 3 **a** Thermogravimetric (TGA) measurements of polymer composite with f-ND and polymer without f-ND; **b** effect of mobile phase flow rate on the pressure of poly(f-ND-co-DPHA-co-EDMA) composite monolith; mobile phase: *a* water and *b* methanol

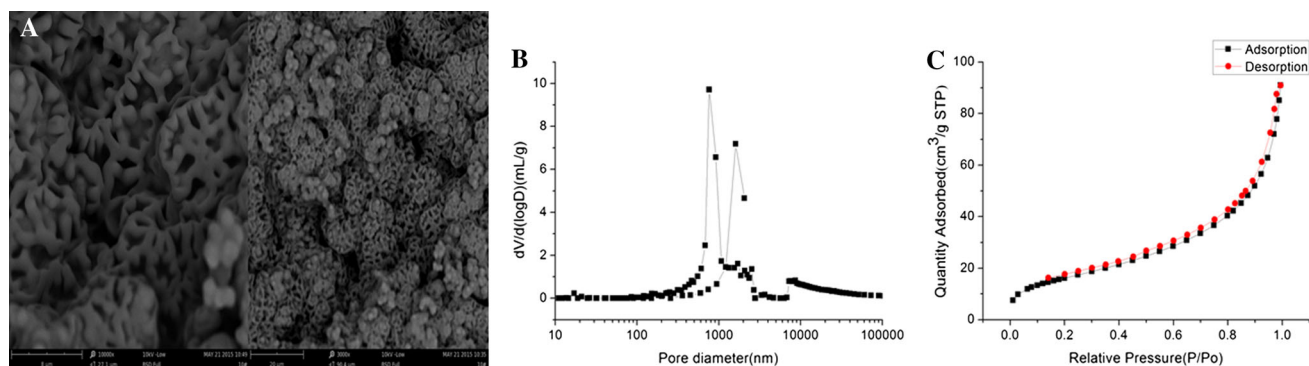


Fig. 4 **a** Scanning electron microscopy of f-ND based composite; **b** the measurement of pore size distribution for f-ND based composite by mercury intrusion porosimetry; **c** nitrogen adsorption–desorption isotherm of f-ND based composite

1.61 μm for the flow-through channels between aggregates of globules and 0.76 μm for the macroporous on those aggregates globules. And the total intrusion volume (2.77 mL g^{-1}), median pore diameter (0.95 μm) and the porosity (74.28 %) were given, simultaneously.

The existence of flow-through channels decreased backpressure along columns and macroporous increased both of orderliness and the specific surface area of materials. The order skeleton structure mentioned above improved the controllability of composite monolithic column, and so does the reproducibility.

Nitrogen adsorption was extensively used for the determination of porous properties of the composite and it allowed a useful estimate of the expected total surface areas of porous polymer composite. As shown in Fig. 4c, the nitrogen adsorption–desorption isotherm exhibited typical type-II hysteresis which indicated the strong interaction between adsorption material and adsorbent. The total surface area of f-ND based polymer composite was found to be $59.6 \text{ m}^2 \text{ g}^{-1}$ from the BET plots, which was higher than that obtained from the polymer without f-ND ($26.3 \text{ m}^2 \text{ g}^{-1}$) added.

3.3 Chromatographic performance

3.3.1 Separation of neutral compounds

In order to investigate chromatographic properties of the poly(f-ND-co-DPHA-co-EDMA) composite monolith, three neutral compounds (benzene, biphenyl and phenanthrene) were used as test compounds. As illustrated in Fig. 5a, benzene, biphenyl and phenanthrene were eluted in order based on their hydrophobicity, confirming reversed-phase separation mechanism. To investigate the effect of f-ND particles on the chromatographic performance, a poly

(DPHA-co-EDMA) monolith was also prepared in the absence of f-ND by using the same preparation procedure as described above. A baseline separation of three benzene derivatives without obvious peak tailing was observed when using the poly (f-ND-co-DPHA-co-EDMA) composite monolith, which was better than that obtained on the poly (DPHA-co-EDMA) monolith. Furthermore, the f-ND based composite monolith exhibited higher column efficiency under the same chromatographic condition in comparison with the poly (DPHA-co-EDMA) monolith. The result suggested further potential of the novel composite monolith for efficient separation of other small molecules. Figure 5b showed that the k of three compounds decreased with increasing content of methanol in the mobile phase from 70 to 90 % (v/v), validating a typical reversed-phase HPLC retention mechanism existed in the poly (f-ND-co-DPHA-co-EDMA) composite monolith.

3.3.2 Separation of different types of compounds by poly (f-ND-co-DPHA-co-EDMA) composite monolith

To further evaluate the separation ability of other small molecules, the poly (f-ND-co-DPHA-co-EDMA) composite monolith was used to separate alkaline substances, phenols. Figure 6a illustrated that the baseline separation of four alkaline compounds was obtained within 7 min. Figure 6b showed the separation of acidic compounds on the composite monolith. As expected, the compounds were eluted in accordance with their hydrophobicity.

Moreover, eight analytes containing alkaline, acidic and neutral compounds have been separated within 17 min in Fig. 6c. Chromatographic parameters such as retention time and resolution, asymmetry factor and theoretical plate number were calculated for each sample and the results were shown in Table 2.

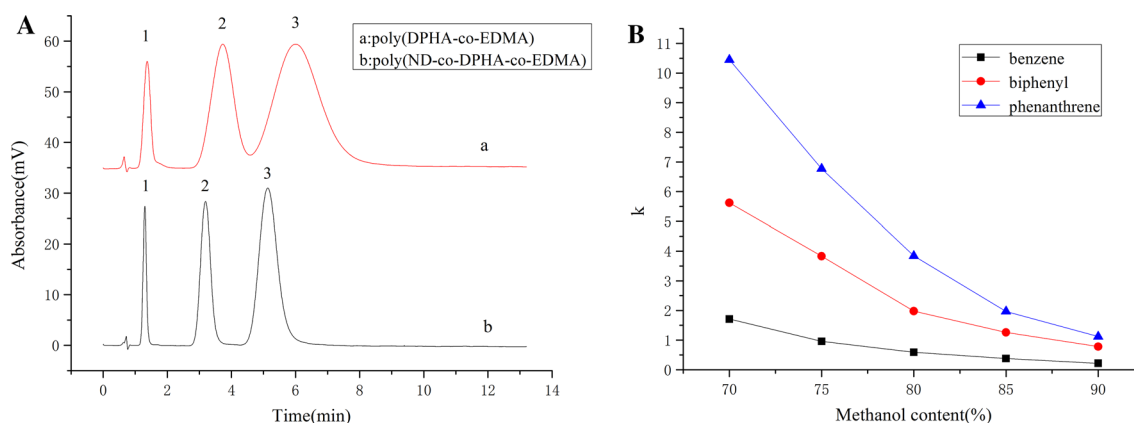


Fig. 5 **a** Separation of benzene, biphenyl and phenanthrene in order with the poly(DPHA-co-EDMA) monolith (*a*) and poly(f-ND-co-DPHA-co-EDMA) composite monolith (*b*); separation condition: methanol/water (70/30, v/v) at a flow rate of 1 mL/min; detection

wavelength, 254 nm. **b** Relationship between retention factor and methanol concentration of neutral compounds on the poly(f-ND-co-DPHA-co-EDMA) composite monolith (column **b**)

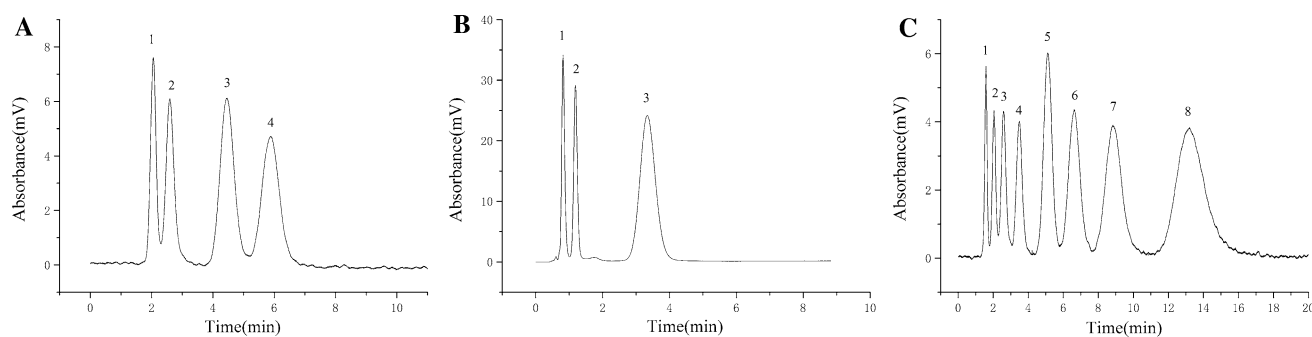


Fig. 6 **a** Separation of four alkaline compounds on poly(f-ND-co-DPHA-co-EDMA) composite monolith in HPLC; separation condition: methanol/water (70/30, v/v) at a flow rate of 1 mL/min; detection wavelength, 254 nm; the analytes were (1) p-nitroaniline (2) aniline (3) p-aminodiphenylimide (4) diphenylamine; **b** separation of three acidic compounds; the analytes were (1) 1,2-benzenediol (2)

phenol (3) α -naphthol; the experimental conditions are the same to the former; **c** separation of eight analytes; the analytes were (1) o-nitrobenzoic acid (2) p-nitroaniline (3) 1-naphthylamine (4) naphthalene (5) diphenyl (6) fluorine (7) phenanthrene (8) triphenylamine; the experimental conditions are the same to the former

Table 2 Chromatographic parameters of separation of small molecules in Fig. 6c

	Retention time (min)	Resolution	Asymmetric factor	Plate numbers (plates per m)
o-nitrobenzoic acid	1.587	1.55	0.94	16,120
p-nitroaniline	2.050	1.45	0.96	14,620
1-naphthylamine	2.595	1.64	1.11	13,280
Naphthalene	3.488	2.15	1.05	13,160
Diphenyl	5.098	1.47	1.03	12,360
Fluorine	6.623	1.56	1.15	11,900
Phenanthrene	8.838	1.93	1.07	11,100
Triphenylamine	13.205		1.09	9798

3.4 Repeatability and stability

The repeatability of poly (f-ND-co-DPHA-co-EDMA) composite monolith production was assessed by measuring the relative standard deviations (RSDs) of *k* values. The RSD of the *k* values were less than 1.47 % (*n* = 6), demonstrating the excellent run-to-run repeatability. Besides, good column-to-column reproducibility of the *k* values was also obtained with RSD less than 2.04 % (*n* = 6). The result suggested that the method had a good reproducibility and the columns were stable.

4 Conclusions

With ND modified with KH570 prepared in our lab, the poly (f-ND-co-DPHA-co-EDMA) composite monolithic column was prepared by one-step redox initiation. In comparison with poly (DPHA-co-EDMA) monolithic column, better mechanical stability, uniform skeleton structure, repeatability and stability were exhibited for the composite ones. More importantly, the f-ND based composite monolith exhibited higher column efficiency due to its bigger surface area. The resulted nanodiamond-based

composite monolithic column was used to separate a series of small molecules including acidic, alkaline and neutral compounds achieving good performance without buffer.

Acknowledgments The study was funded by the National Natural Science Foundation of China (No. 21175031, 21575033, 21505030), the Natural Science Foundation of Hebei Province (No. B2013201082, B2015201024) and the Natural Science Foundation of Hebei University (No. 2014-05).

Compliance with ethical standards

Conflict of interest The authors declare that they have no conflict of interest.

Ethical approval This article does not contain any studies with human participants or animals performed by any of the authors.

References

1. D. Bitounis, H. Ali-Boucetta, B.H. Hong, D.-H. Min, *Adv. Mater.* **25**, 2258 (2013)
2. L. Lacerda, A. Bianco, M. Prato, K. Kostarelos, *Adv. Drug Deliv. Rev.* **58**, 1460 (2006)
3. Y. Li, Z. Zhu, J. Yu, B. Ding, *ACS Appl. Mater. Interfaces* **7**, 13538 (2015)
4. A. Krueger, *J. Mater. Chem.* **18**, 1485 (2008)

5. V.N. Mochalin, L. Neitzel, B.J.M. Etzold, A. Peterson, G. Palmese, Y. Gogotsi, *ACS Nano* **5**, 7494 (2011)
6. P. Badziag, W.S. Verwoerd, W.P. Ellis, N.R. Greiner, *Nature* **343**, 244 (1990)
7. A. Krueger, *Chem. Eur. J.* **14**, 1382 (2008)
8. A. Krueger, *J. Mater. Chem.* **21**, 12571 (2011)
9. V.N. Mochalin, O. Shenderova, D. Ho, Y. Gogotsi, *Nat. Nanotechnol.* **7**, 11 (2012)
10. R. Kaur, I. Badea, *Int. J. Nanomed.* **8**, 203 (2013)
11. M.A.A. Mamun, Y. Soutome, Y. Kasahara, Q. Meng, S. Akasaka, A. Fujimori, *ACS Appl. Mater. Interfaces* **17792**, 7 (2015)
12. T. Jiang, K. Xu, *Carbon* **33**, 1663 (1995)
13. V. Mochalin, S. Osswald, Y. Gogotsi, *Chem. Mater.* **21**, 273 (2009)
14. A. Krueger, D. Lang, *Adv. Funct. Mater.* **22**, 890 (2012)
15. K.D. Behler, A. Stravato, V. Mochalin, G. Korneva, G. Yushin, Y. Gogotsi, *ACS Nano* **3**, 363 (2009)
16. C. Lin, C. Lin, H. Chang, M. Su, *J. Phys. Chem. B* **119**, 7704 (2015)
17. R. Wu, L. Hu, F. Wang, M. Ye, H. Zou, *J. Chromatogr. A* **1184**, 369 (2008)
18. E.F. Hilder, F. Svec, J.M.J. Fréchet, *J. Chromatogr. A* **1044**, 3 (2004)
19. M. Dong, M. Wu, F. Wang, H. Qin, G. Han, J. Dong, R. Wu, M. Ye, Z. Liu, H. Zou, *Anal. Chem.* **82**, 2907 (2010)
20. L. Bai, H. Liu, Y. Liu, X. Zhang, G. Yang, Z. Ma, *J. Chromatogr. A* **1218**, 100 (2011)
21. Q. Gai, F. Qu, Z. Liu, R. Dai, Y. Zhang, *J. Chromatogr. A* **1217**, 5035 (2010)
22. M. Ding, R. Zheng, H. Peng, *J. Anal. Chem.* **37**, 395 (2009)
23. P.A. Bristow, J.H. Knox, *Chromatographia* **10**, 279 (1977)
24. P.S. Nikam, L.N. Shirsat, M. Hasan, *J. Chem. Eng. Data* **43**, 732 (1998)
25. G. Ping, L. Zhang, L. Zhang, W. Zhang, P. Schmitt-Kopplin, A. Kettrup, Y. Zhang, *J. Chromatogr. A* **1035**, 265 (2004)